

Scattering induced dynamical entanglement and the quantum-classical correspondence

M. Lombardi and A. Matzkin

Laboratoire de Spectrométrie physique (CNRS Unité 5588),

Université Joseph-Fourier Grenoble-1,

BP 87, 38402 Saint-Martin, France

Abstract

The generation of entanglement produced by a local potential interaction in a bipartite system is investigated. The degree of entanglement is contrasted with the underlying classical dynamics for a Rydberg molecule (a charged particle colliding on a kicked top). Entanglement is seen to depend on the classical dynamics in a nontrivial manner for two reasons. First system specific terms (such as an anomalously high entanglement due to a kinematic effect) appear to overshadow any putative universal behavior. Second, quantum effects (such as revivals) which are expected to persist in the semiclassical limit rule the long time behavior of the reduced linear entropy. These results suggest that entanglement may not be a pertinent universal signature of chaos.

PACS numbers: 03.65.Ud, 05.45.Mt, 34.60.+z, 03.67.Mn

Entanglement, i.e. the nonseparability intrinsic to composite systems, is one of the most peculiar features of the quantum world. In its most popular form, found for example in the original EPR proposal [1], the entanglement is of geometrical nature. However any usual potential interaction between two particles can generically lead to entanglement, provided several quantum states are accessible to both particles. The study of such dynamical entanglement is particularly interesting for systems which possess a classical counterpart. Recent investigations have been focusing on the relation between the generation of entanglement and the underlying classical dynamics. Initial work in spin-boson systems [2] and in coupled kicked tops [3] suggested that chaotic dynamics generate more and faster entanglement, but this claim was subsequently revised [4, 5, 6], in part due to discrepancies regarding the derivation of the classical limit [7]. Concurrently efforts are being made to derive universal relations ruling the generic generation of entanglement, irrespective of system specifics [8, 9, 10], but the predicted results differ according to the method employed and the approximations made. Thus, contrarily to the well established quantum-classical correspondence for spectral statistics and large scale fluctuations [11], an analog correspondence and the existence of universal regimes regarding the generation of entanglement is still debated and has recently been questioned [12].

In this work we study the generation of entanglement for a real system which possesses an unambiguous classical counterpart. This will be done by employing a bipartite system where entanglement is produced by a local interaction, viz. the particles interact via a short-range scattering potential. We will see that the underlying classical dynamics is reflected in the generation of entanglement, but the quantum-classical correspondence is upset by specific quantum effects, that can nevertheless be understood by appealing to semiclassical arguments. For example we will see that the linear entropy can in certain circumstances rise well beyond the value expected for a maximally mixed state.

The system investigated here is a Rydberg molecule. Simply stated, a Rydberg molecule is composed of two parts: a highly excited electron on the one hand, and a compact ionic molecular core, containing the nuclei and the tightly bound other electrons on the other. Most of the time, the outer electron and the core are spatially well-separated: the core rotates freely with angular momentum N and energy $E_N^+ \sim N^2$, whereas the outer electron senses a pure Coulomb field. Its orbital angular momentum L is fixed in space. Seen in the molecular frame L turns around the N axis (with polar angles θ and θ' , see Fig.

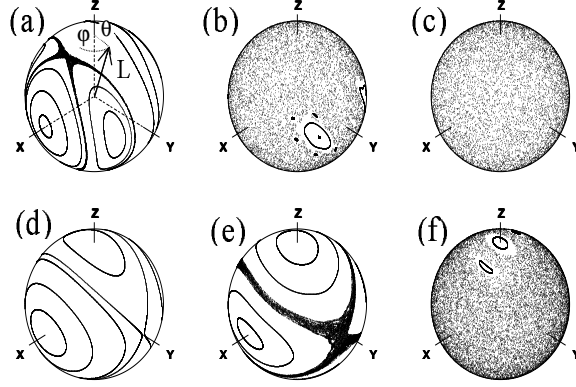


FIG. 1: Poincaré surfaces of section in the molecular frame. The core axis is along OZ and N along OX . Top row: generic case, (a): $k = 0.25$, (b): $k = 1$, (c): $k = 10$. Bottom row: same values of k for the resonant case $T_e = T_0$. (a) also shows the angles θ and ϕ for a given position of L on the sphere.

1(a)). However, the outer electron periodically scatters on the molecular core. Classically the electron is kicked by the rotating core. This kick results in a change in the direction of L by θ' , the deflection angle of the plane of the classical Kepler orbit. N adjusts accordingly, since the total angular momentum $J = L + N$ is conserved. The conservation of L and the cylindrical symmetry of the core implies that $\theta' = k \cos \theta$ where k gives the strength of the kick. A negligibly small kick yields regular dynamics. This is visualized in a Poincaré surface of section obtained by plotting the position of L after each kick (Fig. 1) [13]. For very small k , L encircles the N axis, meaning that L is fixed in space, and thus that on a given circle, the modulus N is constant. As k increases, two cases must be distinguished. In the generic case [Figs. 1(a)–(c)], a chaotic sea progressively takes over until the last islands of regularity disappear. Things are different in the resonant case. Resonances appear when the orbital period of the electron T_e and the rotational period of the core T_0 are commensurate, so resonances are nongeneric. At resonances, chaos is inhibited and only appears along the separatrix [Figs. 1(c)–(f)]. The chaotic sea takes over for values of k larger than in the generic case. Resonances are known to modify the spectrum of small Rydberg molecules, such as the stroboscopic effect experimentally observed on Na_2 [14].

In quantum-mechanical terms the collision couples the electron and core dynamics and induces phase-shifts in the wavefunction of the outer electron. In the absence of the core-electron interaction, the Hamiltonian H_0 is separable and the eigenstates are given by the

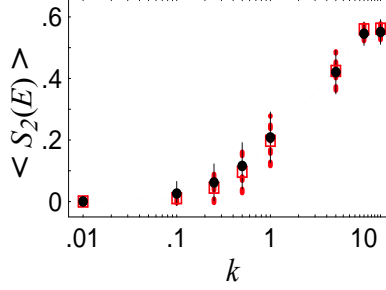


FIG. 2: Average linear entropy for generic (red/gray boxes) and resonant (black dots) states ($T_e = T_0$), shown for different values of k . The rms is also shown as red dashed (generic) and solid (resonant) error bars.

product state

$$\chi_N(E; r) = f_L(E - E_N^+; r) \chi_N^i \quad (1)$$

where E is the total energy, χ_N^i the state of the core and f_L the radial Coulomb function of the electron whose energy is $E - E_N^+$ [15]. The total Hamiltonian $H = H_0 + V$ includes the core-electron interaction potential V . The eigenstates are given from scattering theory by

$$\chi(E; r) = \sum_N Z_N(E) [I + G_0(E)K] \chi_N(E; r); \quad (2)$$

where G_0 is the Green's function, Z_N are expansion coefficients and K is the scattering matrix, whose elements $K_{N_0 N}$ are related to the transition probability amplitude between states N and N_0 due to the collision. From Eq. (2) it is apparent that an eigenstate is given by a superposition of core states with rotational number N , each core state being associated with an outer electron having an energy $E - E_N$. The relation between the quantum and classical pictures is simpler [13] when expressed in the molecular frame, where K has only diagonal elements $\tan \delta$. The phase shifts δ only depend on the coupling between L and the molecular axis. $L_{\parallel} = L \cos \theta$ is the projection of L on this axis and the classical deflection angle is related to the quantum phase shifts by

$$\delta' = 2 \frac{\partial \delta}{\partial L_{\parallel}} = k \frac{\partial \delta}{\partial L}; \quad (3)$$

The first equality is a very general result stemming from the semiclassical approximation to scattering theory [16] and is valid to first order in \hbar , whereas the last term follows from the functional relation $\delta(k)$ chosen in this work which turns out to be verified for typical diatomic molecules.

To quantify entanglement we will compute the linear entropy S_2 associated with the reduced density matrix describing the electron

$$S_2 = 1 - \text{Tr} \rho_e^2; \quad (4)$$

where $\rho_e = \text{Tr}_c \rho$ and as usual Tr_c (Tr_e) refers to averaging over the core (electron) degrees of freedom. We first determine the degree of entanglement of stationary states. This is done by calculating $\langle S_2(E) \rangle = \langle -\log_2 \text{Tr} \rho_e^2(E) \rangle$ over an energy range for which the classical dynamics does not vary appreciably. The values $L = 2$ and $J = 10$ adopted in this work correspond to experimentally accessible values for diatomic molecules such as Na_2 . With these values and taking into account symmetry requirements, three rotational states are accessible to the core $N = 8; 10; 12$ (classically, $8 \leq N \leq 12$). Hence in a typical eigenstate ρ three core-electron states are entangled. The mean entropy $\langle S_2(E) \rangle$ for stationary states is shown in Fig. 2 as a function of the coupling constant k . The curves for the generic and resonant cases are very close despite phase-space being substantially different for most values of k . On average the potential interaction entangles at least as efficiently when the underlying classical dynamics is mostly regular rather than mainly chaotic. Note the rms is small for the regular and totally chaotic regimes and larger in the mixed phase-space situation and that the linear entropy saturates in both the generic and resonant cases only for large k : $\langle S_2(E) \rangle$ approaches its upper limit $2=3$ corresponding to a maximally mixed state.

We next determine the time-dependent generation of entanglement from an initial product state. At $t = 0$ we take the wavefunction of the electron to be radially localized at the outer turning point r_{tp} , several thousand atomic units away from the core, and we take the core to be in the rotational state $|N_0\rangle$, so that

$$\psi(t=0; r) = F_{loc}(r - r_{tp}) |N_0\rangle; \quad (5)$$

The mean energy of the radial wavepacket F_{loc} is $E_0 = E_0 - E_{N_0}^+$ and T_e is the period of the corresponding Kepler orbit. At $t = T_e/2$ the wavepacket scatters off the core and the wavefunction is given by a superposition of radial wavepackets moving outward, each associated with a core in a given rotational state $|N\rangle$. At $t = T_e$ each of the radial wavepackets has reached the outer turning point and starts going back towards the core. The core-electron interaction then takes place again at $t = 3T_e/2$ resulting in further entanglement change. As t increases the wavepackets tend to spread radially resulting in a continuous core-electron

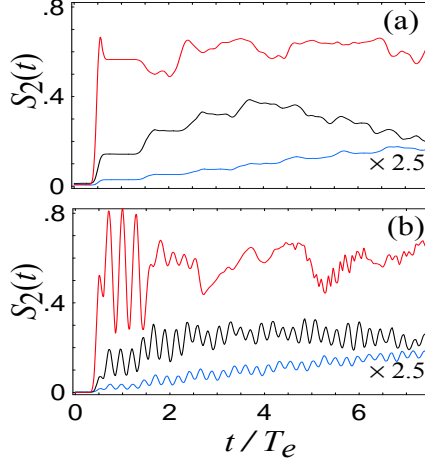


FIG. 3: Short time variation of the linear entropy for different values of the coupling strength; t is given in units of the Kepler period T_e . (a) Generic phase-space, from top to bottom $k = 10$ (red), 1 (black) and 0.25 (blue). The $k = 0.25$ curve is multiplied by a factor 2.5. (b) Same as (a) for the resonant case $T_e = T_0$.

interaction. These features appear in the time dependence of the linear entropy $S_2(t)$, obtained from Eq. (4) by tracing out the core degrees of freedom from the total density matrix $\rho_j(t) = \text{tr}_c(\rho_{ij}(t))$.

For short times $S_2(t)$ is shown in Fig. 3, for $N_0 = 12$ and for 3 different values of the coupling k . In the generic case, for small t and not too large k , S_2 is seen to increase in steps, reflecting the discrete times core-electron interaction. In this regime, a semiclassical approximation to the purity $\text{Tr}_e \rho_e^2$ predicts that $S_2(t_c) \sim k^2 t_c$. This result, valid only for the collision times $t_c = (2m + 1)T_e = 2$, is obtained in the stationary phase approximation by neglecting correlations between electron orbits built on different core rotational states. The k^2 dependence comes from the semiclassical amplitudes, and the linear variation in t from the fact that these amplitudes are conserved. For longer times, S_2 appears to saturate (but see below). An analog behavior is seen in the resonant case. Note that for $k = 0.25$ the linear entropy saturates at a similar value in the generic and resonant cases while phase-space in both cases is mostly regular (see Fig. 1); for $k = 1$ $S_2(t)$ saturates at a lower value in the resonant case, while phase space in the generic case is more chaotic than in the resonant case. This is to be contrasted with the value of $\langle h S_2(E) \rangle$ which is nearly identical for generic and resonant states, as seen in Fig. 2.

However the striking difference between the generic and resonant cases concerns the large

amplitude oscillations of S_2 in the latter case. For example for $k = 0.25$; S_2 is seen to increase on average linearly in time, but oscillates around the average with a period $T_0=4$. This is a quantum kinematical effect, due to the resonance, that can be understood semiclassically in the following way: assuming the coefficients $Z_N(E)$ in Eq. (2) are on average nearly equal (which is approximately realized for resonant states) the purity is seen to depend on the square of

$$\sum_{N \neq N'} \sum_{E \neq E'} e^{i(E - E')t} hF_L^{(0)}(N) jF_L^{(0)}(N'); \quad (6)$$

where $\epsilon = E - E'$ depends on N ; and $F_L^{(0)}(r)$ are radial functions on the energy shell (i.e. a combination of regular and irregular Coulomb functions with effective phase shifts depending on the scattering matrix K). These functions are not orthogonal in r although the overlap is negligible when $j \neq j'$. Expanding the core energies in the exponential to first order and using the WKB quantization condition leads to

$$\sum_{N \neq N'} e^{2i t[(N - N') = T_0]} \sum_{(N')^{(0)}(N^{(0)})} e^{i(\epsilon^{(0)})t} hF_L^{(0)}(N) jF_L^{(0)}(N'); \quad (7)$$

In the generic case the second sum yields except accidentally small terms (since the overlap usually vanishes) and there is no correlation between each of these terms. This is no longer the case when the resonance condition is satisfied because the spacings of the core and electron energies coincide. Then $\epsilon^{(0)} = 2m\pi = T_e$, T_e being a multiple of T_0 , and there are energies in the sum (6) for which the overlap is nearly unity. In Fig. 3 (b) we have $T_e = T_0$ so that the exponentials give overall an oscillation with a period $T_0=2$; which when squared is in agreement with the observed $T_0=4$ period. We have coined the label kinematical to these oscillations because they do not correspond to a dynamical effect in the wavefunction or in the probability flux. Indeed, these oscillations are present irrespective of the underlying classical dynamical regime. This kinematical effect accounts for the otherwise surprising observation for the $k = 10$ linear entropy, which is pushed well above its expected maximum value of $2=3$ corresponding to maximally mixed states.

The long time behavior of the entanglement production is shown in Fig. 4. In the generic case, periodic recoherences are readily visible for small k . Although revivals are expected when phase space is regular and the dimensionality of the Hilbert space is low, we point out that the same observations have been made for considerably larger angular momenta closer to the semiclassical limit [17]. Similar long time recoherences with no classical counterpart

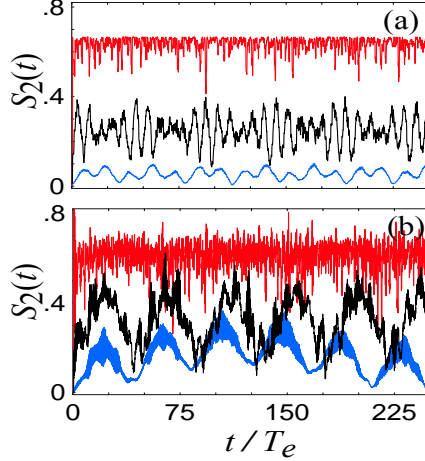


FIG. 4: Same as Fig. 3 for longer times (the curves for $k = 0.25$ are not multiplied by 2.5). The ‘thick’ aspect of the curves in (b) is due to the short-time oscillations, which are not resolved on the scale of the plot.

were recently observed in a model describing coupled Bose-Einstein condensates [9]. The characteristic periods of recoherence involve the revival times T_0^{rev} and T_e^{rev} of the core rotation and the electron orbit. The former readily appears by carrying the expansion in E_N^+ in Eq. (7) to second order. The latter follows by remarking that the second sum in Eq. (7) is the cross-correlation function between parts of the wavefunction belonging to different superposition alternatives (i.e. different channels). The dependence of T_e^{rev} on the collision channel is considerably more important than for T_0 and T_e , so S_2 is expected to depend on a combination of different time scales. For example for $k = 0.25$ 2 oscillation scales are visible corresponding to T_e^{rev} ($N = 12$) and the longer T_0^{rev} ($N = 10$). In the resonant case the long-range oscillations can be dramatically enhanced by the commensurate time scales (in addition to $T_0 = T_e$, we have $T_0^{\text{rev}} = 2T_e^{\text{rev}}$). As a result the curves for k values corresponding to different underlying classical dynamics cross periodically. It is also instructive to confront classical phase-space with the value of the linear entropy for short times (Fig. 3) and for long times (e.g. for $k = 1$, S_2 grows at first slower in the less chaotic case [Fig. 2(e)] but then oscillates more violently). The visibility of revivals depends on how the relative changes of the net probability flux in each channel are correlated. Hence in a mixed phase-space situation revivals will most easily be seen if the initial wavepacket lies in a regular region, whereas as k increases the mixings become too strong for any fractional revival to be seen, even in systems with a low dimensionality.

To sum up we have investigated the generation of entanglement induced by a potential interaction in a bipartite system, a Rydberg molecule. By and large chaotic classical dynamics is associated with more and faster entanglement but this appears to result from the fact that mixings (ruled in our system by the rate of inelastic scattering) are often facilitated by chaotic dynamics. Hence chaos is neither compelling nor necessarily the most efficient way to ensure mixings. The present observations support similar results obtained for coupled kicked tops [12]. We have also seen the existence of specific effects in the time evolution of the linear entropy, such as the kinematical short time oscillations observed for resonant states and the dynamical long range oscillations arising from partial wavepacket revivals. None of these effects have a classical counterpart. Further studies are needed to determine under which conditions interactions of the system with an environment, such as coherent states of the electromagnetic field, can account for the disappearance of these quantum effects and the appearance of a classical world [18].

We are grateful to T.H. Seligman (UNAM, Cuernavaca, Mexico) for fruitful discussions.

-
- [1] A. Einstein, B. Podolsky and N. Rosen, *Phys. Rev.* 47, 777 (1935).
 - [2] K. Furuya, M. C. Nemes and G. Q. Pellegrino, *Phys. Rev. Lett.* 80, 5524 (1998).
 - [3] P. A. Miller and S. Sarkar *Phys. Rev. E* 60, 1542 (1999).
 - [4] R. M. Angelo et al, *Phys. Rev. A* 64, 043601 (2001).
 - [5] H. Fujisaki, T. Miyadera, and A. Tanaka *Phys. Rev. E* 67, 066201 (2003)
 - [6] M. Novaes and M. A. M. de Aguiar, *Phys. Rev. E* 70, 045201 (R) (2004).
 - [7] J. N. Bandyopadhyay and A. Lakshminarayanan *Phys. Rev. E* 69, 016201 (2004)
 - [8] Ph. Jacquod, *Phys. Rev. Lett.* 92, 150403 (2004)
 - [9] R. M. Angelo and K. Furuya, *Phys. Rev. A* 71, 042321 (2005).
 - [10] M. Znidaric and T. Prosen *Phys. Rev. A* 71, 032103 (2005)
 - [11] F. Haake, *Quantum signatures of chaos* (Springer, Berlin, 2001).
 - [12] R. Demkowicz-Dobrzański and M. Kus *Phys. Rev. E* 70, 066216 (2004)
 - [13] B. Dietz, M. Lombaridi and T. H. Seligman, *Ann. Phys.* 312, 441 (2004). M. Lombaridi et al, *J. Chem. Phys.* 89, 3479 (1988).
 - [14] P. Labastie et al, *Phys. Rev. Lett.* 52, 1681 (1984); E. S. Chang et al. *J. Chem. Phys.* 111,

6247 (1999).

[15] The angular part of the electron wavefunction is contained in the compound notation \mathcal{N}^i due to the coupling of angular momenta. This 'geometrical entanglement' plays no role in this work which focuses on the superpositions in \mathcal{N}^2 and not in the relative orientations of the angular momenta.

[16] R. G. Newton, *Scattering theory of waves and particles* (Springer, New York, 1982), Ch. 18.

[17] M. Lombardi and A. Matzkin, in preparation.

[18] W. H. Zurek *Rev. Mod. Phys.* 75, 715 (2003)